Progress In Electromagnetics Research B, Vol. 32, 243–262, 2011

LOW-LEAKAGE WITH ATTENUATED MATERIAL LOSS HYBRID COAXIAL CABLE

D. Elbaz and Z. Zalevsky*

School of Engineering, Bar-Ilan University, Ramat-Gan 52900, Israel

Abstract—We investigate a new mean of decreasing leakage and material loss from coaxial cables using different metallic shield and central conducting part geometries. The suggested model is composed of a central conductor surrounded by 40 metallic wires circularly disposed. The proposed cable is also a hybrid one allowing simultaneous transmission of optical as well as radio frequency (RF) signals. The fabrication techniques for the proposed cable are similar to the one applied in the realization of optical fibers. Besides the fact that the attenuation along the proposed cable is reduced, the most important result of this study is that the interference generated by this source on external cables is also lowered.

1. INTRODUCTION

Coaxial cables are often used to transmit radio frequency (RF) signals. These frequencies, which can vary from 3 kHz to 300 GHz, can be useful for very specific tasks like military applications or as an ultrasound scanning equipment. They can provide our daily needs as internet access or video and radio broadcasting.

Many studies have been carried out concerning the behavior of those types of cables. Mathematical models for characterizing a braided cable shield through its transfer impedance were developed in [1, 2]. Loss considerations and cable shield effectiveness were studied in [3–5]. Thermal losses arising from the skin effect phenomenon were analyzed [6] and measured in the case of coaxial cables [7, 8]. New methods for evaluating the transient behavior of coaxial cables using skin effect approximation were presented in [9] and later on extended in [10–12].

Electromagnetic leakage can be caused, among other things, by the structure of the metallic shield, more precisely its holes [13], or by

Received 31 May 2011, Accepted 11 July 2011, Scheduled 18 July 2011

* Corresponding author: Zeev Zalevsky (zalevsz@biu.ac.il).

its asymmetry relatively to the central conducting region and which results from technological fabrication limitations [14].

From the realization point of view, full symmetry is actually not achievable. On the other hand, using technologies developed for optics communication, one may produce in-fiber nano wires that could solve, to a great extent, this problem [15].

In this paper, we present a new metallic shield design that can be fabricated using the fiber fabrication techniques taken from optics communication and which could solve this technological-related asymmetry problem.

A unique central wire will also replace the group of wires generally used in classical coaxial cables in order to reduce thermal losses.

In addition, the same cable can be used to transmit a hybrid type of signals, i.e., not only RF but optical as well. This structure could then be used as an alternative to optically transmitted RF signals [16]. This structure could indeed allow the transmission of hybrid signals without the need to convert an electrical signal to its optical equivalent or vice versa [17–19]. It could also be a mean to transmit an RF signal at a relatively low cost by using the fabrication techniques for optical fibers while classical RF cables and many more hybrid fiber optic/electrical cables [20] are relatively expensive to fabricate.

In Section 2, we present the design considerations while the simulations and the performance characterization are brought in Section 3. Fabrication considerations are reported in Section 4. The paper is concluded in Section 5.

2. DESIGN CONSIDERATIONS

The cross section for the proposed model is depicted in Fig. 1. The latter is built up by a copper-made central core having a radius of 0.39 mm. This one is encircled by 40 wires made from the same material and which play the role of the shield. Having a radius of 0.09 mm, these peripheral wires are distanced from the cable center a distance of 1.22 mm. The metallic part is strengthened by a silica-glass-made one that has good dielectric properties. The proposed structure has a total diameter of 4.4 mm.

This model will be compared with a modeled classical coaxial cable which has almost the same characteristics as RG-58 cable, except one detail: its external layer is made from silica glass rather than from plastic (see Figs. 2(a) and 2(b)).

The reason of this choice is due to our desire to exclusively study the impact of the new structure that includes conducting parts (not only the cable shield but also the central core which is now composed

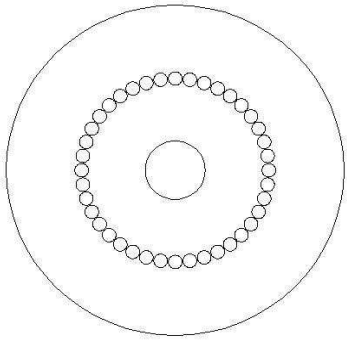

Figure 1. The cross section of the studied structure.

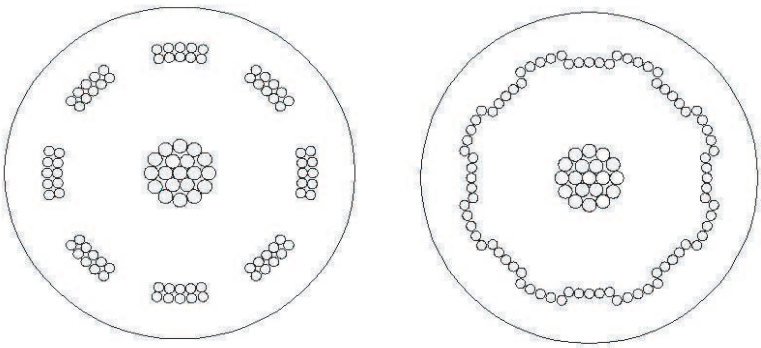

Figure 2. The coaxial like cable cross sections for (a) a metallic shield exhibiting its largest apertures (first cross section) or (b) covering totally the central conducting zone (second cross section).

of only one metallic wire) on the magnetic leakage and the thermal losses. Indeed, the compared cables have, for both the central part as well as for the shield, the same cross section area. The external diameter of the two structures is also the same and it is 4.4 mm.

Because of the fact that, in a classical coaxial cable, the metallic shield cross section depends on the cut plane, we have chosen to simulate its behavior using two characterizing cross sections. The first one represents the case in which the shield exhibits the largest apertures at its periphery (Fig. 2(a)). In the second cross section representation, we have simulated the case in which the two-layers shield covers totally the central wires (Fig. 2(b)).

All the numerical investigations have been performed in two dimensions using COMSOL Multiphysics 3.5. which is a commercial software that solves partial differential equations via the finite elements method.

3. NUMERICAL INVESTIGATION

In our simulations, a current amplitude value of 2.5 A and a frequency varying from 100 MHz to 1 GHz have been used.

3.1. Power Flow Calculation

We have first calculated the time averaged power flow, which can be expressed in the following way:

$$P = \iint \left\| \vec{S} \right\| \cdot ds \tag{1}$$

where $\|\vec{S}\|$ is the norm of the Poynting vector. This value has been calculated in the vicinity of our compared structures: a corona with an external radius of 5 cm.

3.1.1. The Symmetrical Case

First, we calculated the value of P and compared it with our classical coaxial cable model. The results are presented in Figs. 3(a), 3(b) and 3(c). We can see that the proposed structure can give rise to a lower magnetic leakage. These results can be explained by the fact that our model does not exhibit holes and because of a greater proximity of its peripheral wires to the central conducting wire.

However, a remark concerning one of the results has to be made. In Fig. 3(a), a peak is appearing around 230 MHz. Given that copper has no particular behavior around this frequency, this phenomenon could be related to the geometry of the proposed structure. Indeed, the scaling down of the structure dimensions by a factor of 0.8 has shifted this peak to 450 MHz approximately (see Figs. 4(a) and 4(b)).

Taking into account that, technologically speaking, it could be difficult to get shielding wires in contact, we have simulated the case in which the wires' positions are distanced from the center by 10%. Concerning our model, we obtained that the time averaged power flow is varying between 9.47×10^{-20} W (for 100 MHz) and 8.86×10^{-23} W (for 1 GHz) while for the classical coaxial cable having the first cross section the variation is between 1.20×10^{-11} W (for 100 MHz) and 2.86×10^{-13} W (for 1 GHz) and for the cable with the second cross

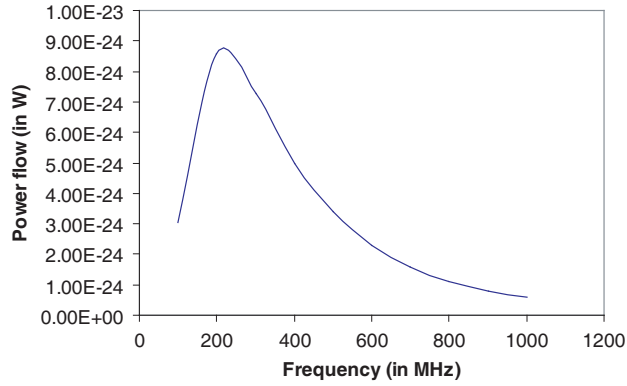

(a)

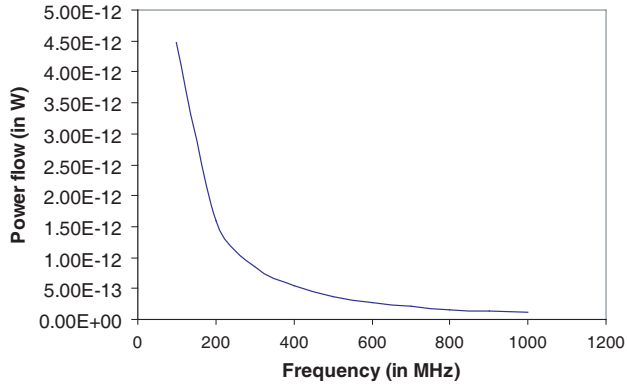

(b)

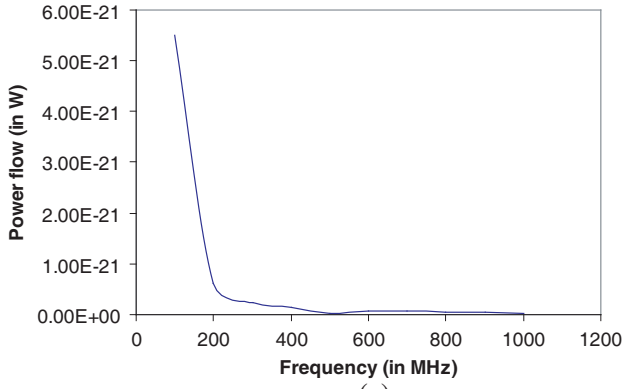

(c)

Figure 3. (a) Time averaged power flow value for the modeled cable, (b) the first cross section coaxial like cable and (c) the second cross section coaxial like cable.

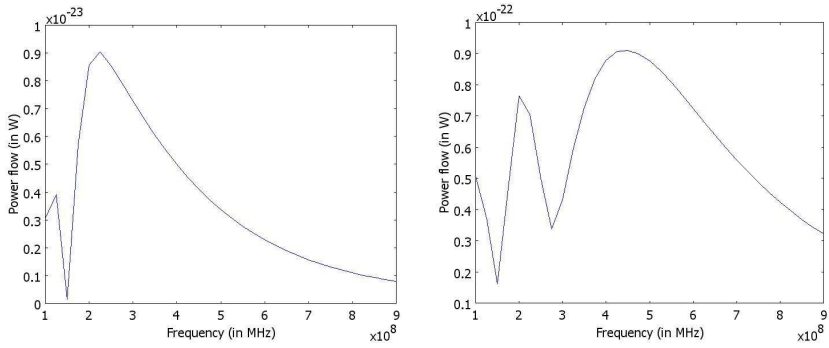

Figure 4. Effect of the cable's dimensions on the power flow peak for (a) the initial scale, (b) a scale factor of 0.8.

section it is between 1.36×10^{-15} W (for 100 MHz) and 1.31×10^{-17} W (for 1 GHz). Remembering that for the case when the peripheral wires of the classical coaxial cable are ideally placed, the time averaged power flow is varying between 4.48×10^{-12} W (for 100 MHz) and 1.09×10^{-13} W (for 1 GHz) for the cable with the first cross section, and between 5.50×10^{-21} W (for 100 MHz) and 2.97×10^{-23} W (for 1 GHz) for the cable with the second cross section. Thus, we can say that even in this case, our proposed model is a good candidate because of the large sensitivity to position existing in conventional cables yielding eventually enormous magnetic leakage when the shield exhibits its larger apertures.

3.1.2. Asymmetry Considerations

As said above, technologically speaking, there are always deviations from perfect symmetric configuration. We tried to simulate this phenomenon using a specific but representative case. We studied the behavior of a metallic shield having its top right hand corner wires that have been moved away from the center by an amount of 5% (see Figs. 5, 6(a) and 6(b)). By calculating also the time averaged power flow of the modified structures, we have obtained the results that appear in Fig. 7.

Despite the fact the generated asymmetry in the two compared structures has the same order of magnitude (technologies developed for optics communication enable us to place the shield wires with a better precision), we can see that the losses remains lower using the proposed configuration.

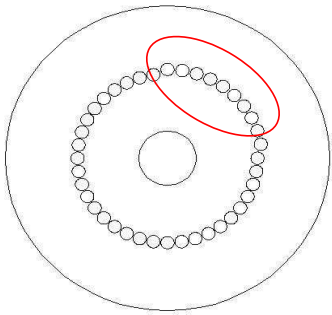

Figure 5. The asymmetric studied model (the red circles point out the wires that generate the shield asymmetry).

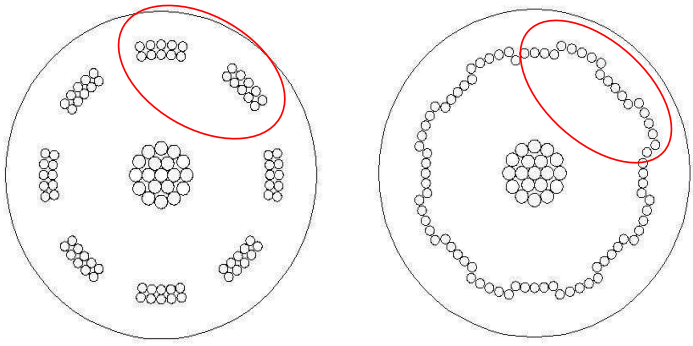

Figure 6. (a) The asymmetric coaxial like cable's cross sections when the metallic shield exhibits its largest apertures or (b) when it totally covers the central wires.

3.2. Electrical Coupling

Another way to quantify the electromagnetic leakage is to evaluate the electrical coupling between two adjacent cables. This has been performed by measuring the current induced from one cable to the next. Even if induced currents are also appearing in the shielding wires, calculations have been restricted to the central conducting wire by integrating the induced current density over its entire surface.

Placing their centers 4.5 mm apart, we have then compared the coupling between two cables having the proposed geometry (see Fig. 8)

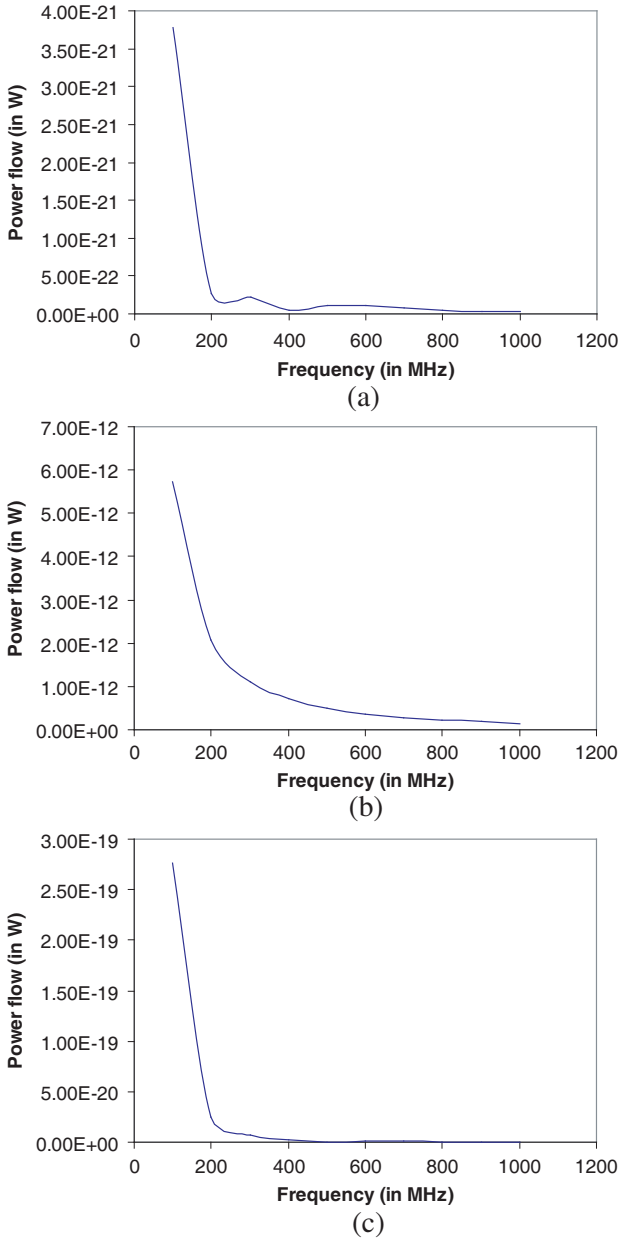

Figure 7. (a) Time averaged power flow value for the asymmetric modeled cable, (b) the asymmetric first cross section coaxial like cable, (c) the asymmetric second cross section coaxial like cable.

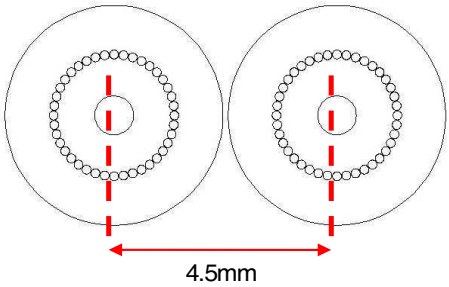

Figure 8. Coupling between two cables having the proposed structure.

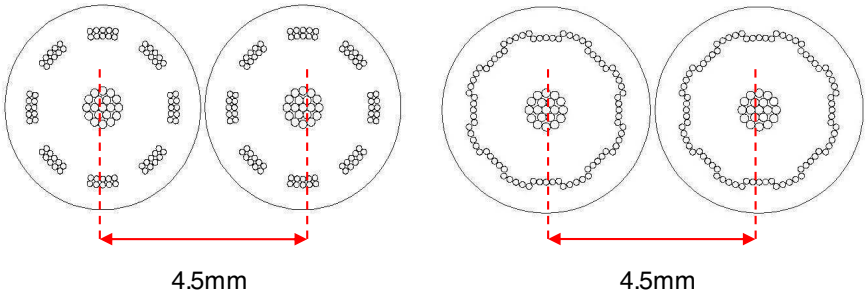

Figure 9. Coupling between two classical coaxial cables: (a) the two shielding layers exhibit the largest apertures at their periphery, (b) the central wires are totally covered.

with the one of two classical coaxial cables. In the last case, the coupling has been studied for two specific cross sections. These cross sections are in fact the two shielding effect limited cases.

In the first situation, the two shielding layers exhibit the largest apertures at their periphery (see Fig. 9(a)). In the second one, the central wires are totally covered (see Fig. 9(b)). In all the following simulations, the induced current is generated in the right cable.

Relatively to the left cable, whatever the configuration is, we have found that the induced currents are practically nonexistent.

For reference only, we have isolated the central conducting wire of the right cable and depicted the induced current density when the coupling concerns two cables having the new structure (Fig. 10) or the classical one (Figs. 11(a) and 11(b)). In these three last figures, the structures were tested at RF frequency of 500 MHz. We can observe that, roughly, the induced current is lowered in our structure.

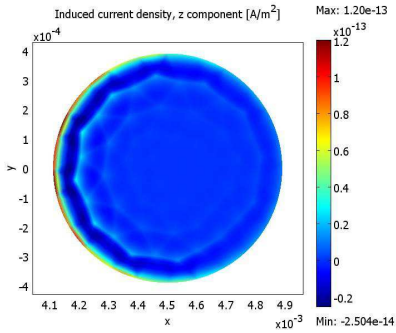

Figure 10. Coupling between two cables having the proposed structure when the frequency equals 500 MHz: the induced current density in the right cable's central conducting wire.

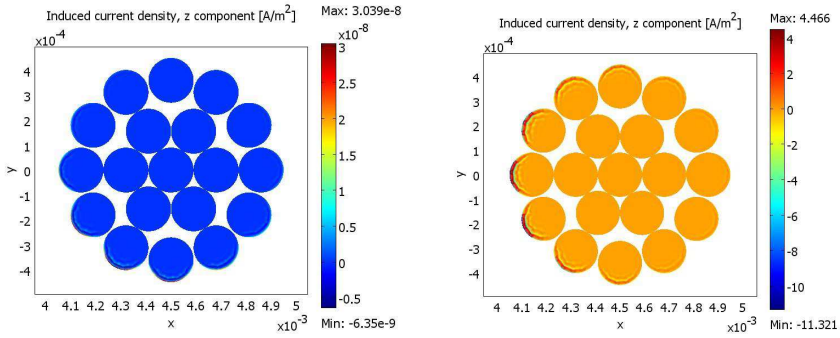

(a) (b)

Figure 11. Coupling between two classical coaxial cables when the frequency equals 500 MHz: (a) the induced current density in the right cable's central conducting wire when the two shielding layers exhibit the largest apertures at their periphery, (b) the induced current density in the right cable's central conducting wire when the central wires are totally covered.

More generally, and for a frequencies range varying from 100 MHz to 1 GHz, we have calculated the total induced current that flows in the central conductor of the right cable and decomposed it into its real and imaginary (related to the signal attenuation) parts. Fig. 12 shows the results obtained for the proposed geometry and Figs. 13 and 14 are presenting the equivalent results for the case of the classical cables. From the simulations we can confirm that when the cables that are in contact are identical, the induced current is lowered in our structure.

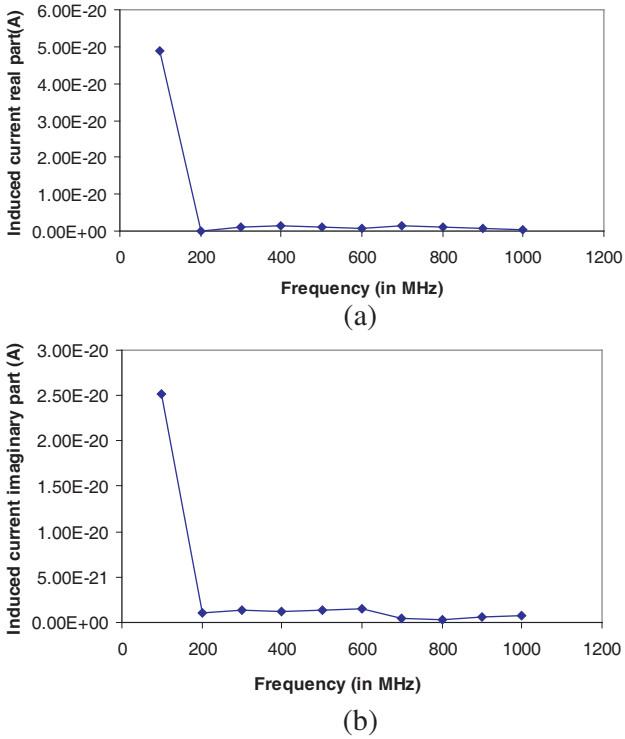

Figure 12. Induced current in the right cable central conducting wire for the proposed model: (a) the real part, (b) the imaginary part.

3.3. Resistive Heating Considerations

In this subsection, we will concentrate on the central conducting zone (which carries the information) for both our proposed model as well as in the classical RG-58 like coaxial cable.

We can comment that between the two structures, the only geometrical difference is the wires number: nineteen in the RG-58 cable and only one in our model. This choice has been motivated by the fact that in AC conditions and due to induction based phenomenon, electrical current flows only through a small thickness of the wire's periphery. Then, when several wires which conduct current in the same direction are in contact, the only zone that is effectively conveying current is the one that is not in proximity to the neighbor wire. By comparing this nineteen wires cross section to a single wire having the same area, we have supposed that the effective surface through which the current could flow would be larger in our model. The effective resistance of the proposed structure would thus be smaller.

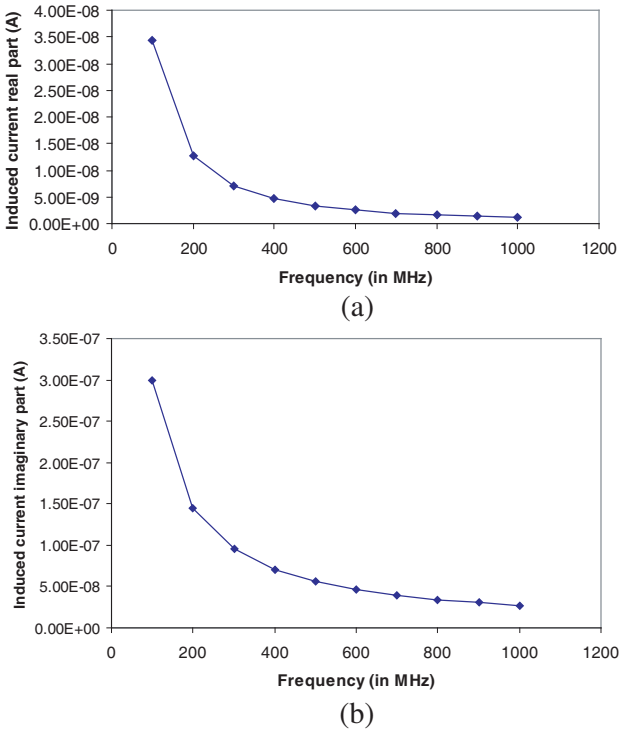

Figure 13. Induced current in the right cable central conducting wire for the classical coaxial structure when the two shielding layers exhibit the largest apertures at their periphery: (a) real part, (b) imaginary part.

Despite the fact that by when replacing nineteen wires by a single one mechanical problems could arise, we can comment that the central conducting wire of the proposed structure has still a smaller radius than the one of RG-59 cables which have a relatively good flexibility.

Thermal losses have been evaluated by measuring the structure resistive heating. Its mathematical expression has the following form:

$$Q = \frac{1}{2}\sigma \left\| \vec{E} \right\|^2 \tag{2}$$

where $\vec{E}$ is the electrical field and σ is the electrical conductivity which equals to:

$$\sigma = \frac{1}{[\rho_0(1 + \alpha(T - T_0))]} \tag{3}$$

with ρ_0 being the resistivity at room temperature T_0 (293 °K), α

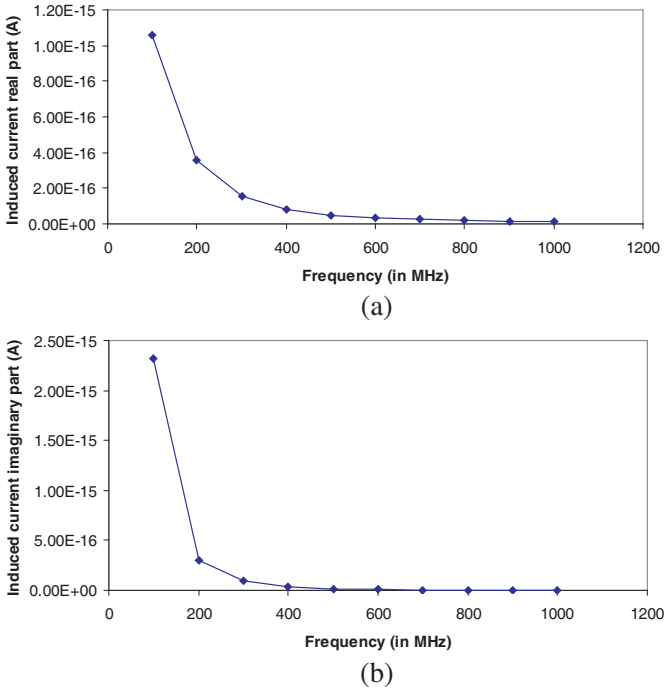

Figure 14. Induced current in the right cable central conducting wire for the classical coaxial structure when the central wires are totally covered: (a) real part, (b) imaginary part.

is the temperature coefficient of the resistivity, and T is the actual temperature.

Quantitatively speaking, we have obtained, for the coaxial cable model and the proposed structure, the results that appear in Fig. 15. In Fig. 16, we have represented the time averaged resistive heating values when asymmetries (see Section 3.1.2) are taken into account. Indeed, simulations confirmed that resistive heating is lowered with our model.

As an example for a frequency of 500 MHz, we have also represented the time averaged resistive heating for our model and the coaxial like cable (see Figs. 17(a), 17(b) and 17(c)).

Note that because in our structure the shield wires are being closer to the central zone, we would have been in right to say that this will badly affect the resistive values in our designs. However, simulations proved that the passage from a multiple wires central core to a single one had a greater impact on the resistive heating than the affect of the increased proximity for the metallic shield.

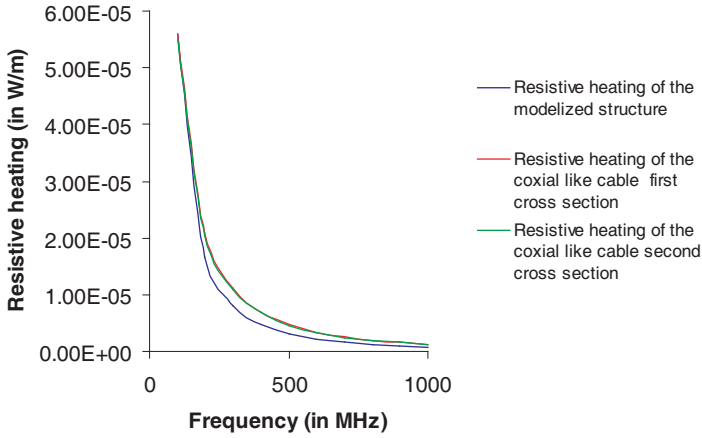

Figure 15. Time averaged resistive heating of the modeled structure (blue line), the coaxial like cable first cross section (red line), the coaxial like cable second cross section (green line).

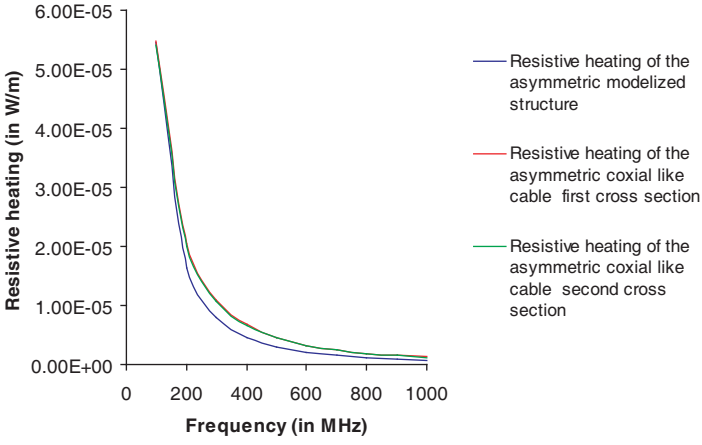

Figure 16. Time averaged resistive heating of the asymmetric modeled structure (blue line), the asymmetric coaxial like cable first cross section (red line), the asymmetric coaxial like cable second cross section (green line).

3.4. Optical Simulations

Given that both the central metallic wire and the peripheral ones are prone to absorb light when exposed to (which is represented via its electrical field in our simulations), we have taken into account this

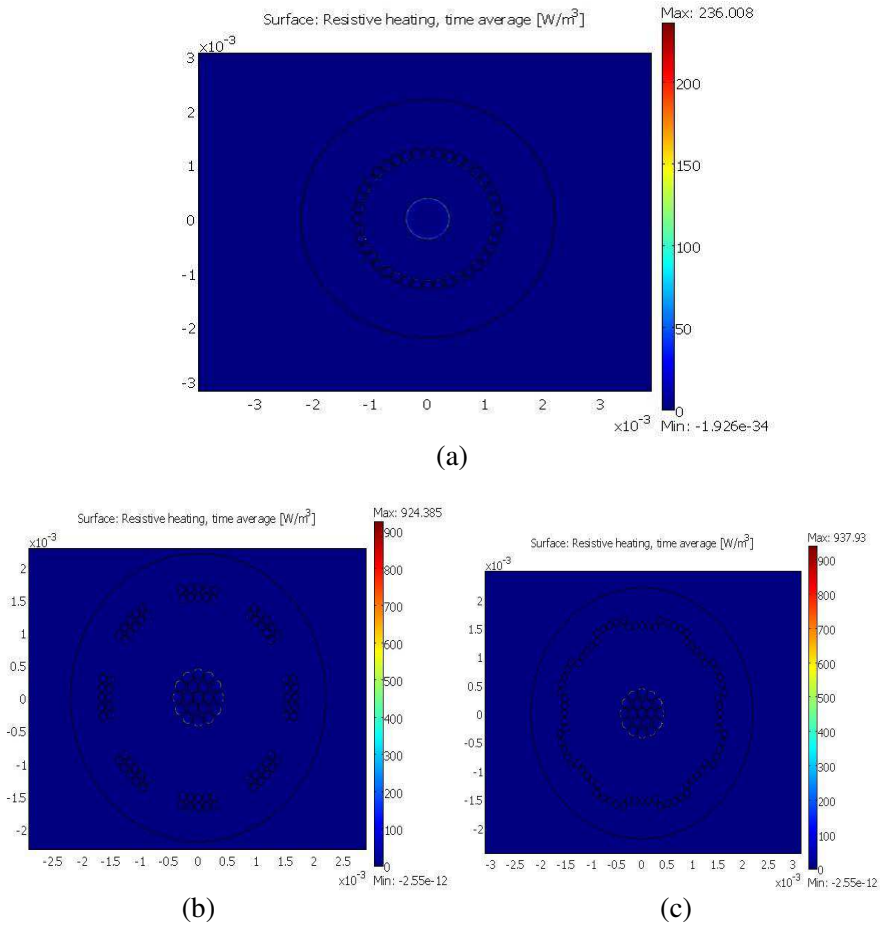

Figure 17. Resistive heating at 500 MHz for (a) the new structure, (b) and (c) versus the traditional coaxial cable at two cross sections. Horizontal units are in meters.

notion in order to place an "optical core" in such a location while the optical loss of such a core would be similar to the losses obtained in classical optical fibers. We are working, for the moment, on a structure that would convey one optical mode only, but yet we have obtained a configuration which allows us to combine an RF signal as well as an optical one.

We based our design on the cross sectional dimensions of the multimode optical fiber, that has a core diameter of about 20 µm and

cladding with diameter of 140 μm. The optical core was then placed in such a location that within a radius of 70 μm, neither copper nor air could be reached.

In our optical simulation the core had refraction index of 1.46 and the cladding of 1.45. The optical wavelength was 1.55 μm. The center of the core of the multimode optical fiber was placed 0.75 mm aside from the center of the proposed cable.

In Fig. 18(a), we show the cross section of the structure containing an optical core conveying an optical mode for wavelength of $\lambda = 1.55\,\mu m$. In Fig. 18(b), a 3D representation of this specific solution is shown. Fig. 18(c) exhibits the electrical field along the line for which

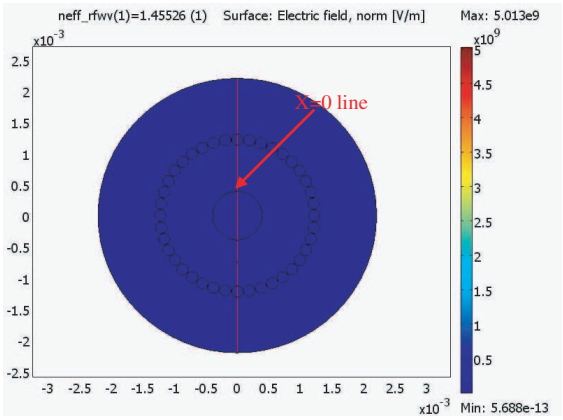

(a)

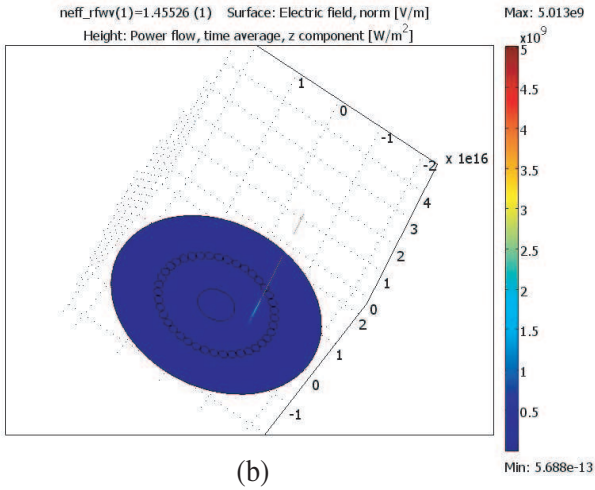

(b)

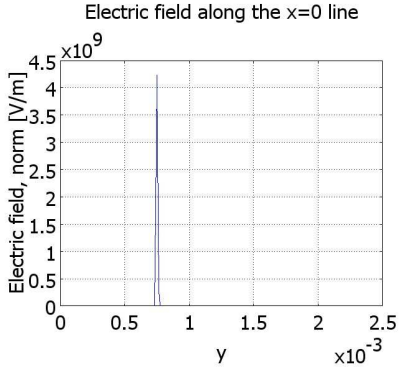

(c)

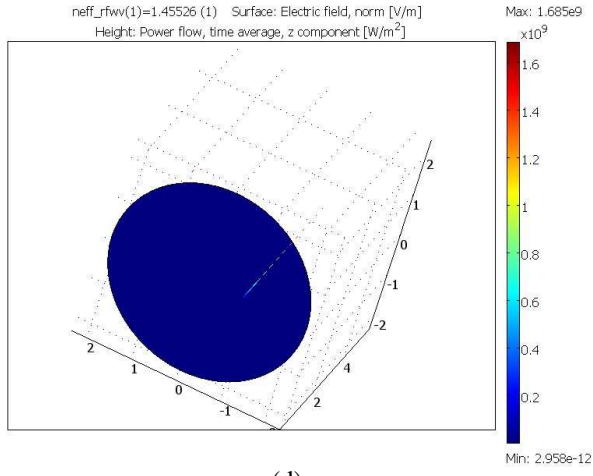

(d)

Figure 18. Optical transmission: (a) The cross section of the structure including an optical core, (b) 3D representation of the mode, (c) Electrical field along the $x = 0$ line, (d) Optical mode without metallic wires.

$x = 0$ (see Fig. 18(a)).

In order to confirm the fact that the optical signal is not influenced by the presence of the electrical wires, we have simulated the case in which no electrical wires are present. We have indeed obtained that the norm of the electric field has the same order of magnitude as the one found in our modeled structure (see Fig. 18(d)).

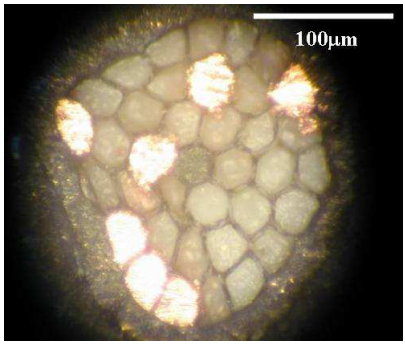

Figure 19. Insertion of plurality of golden wires into a photonic crystal pre-form using a drawing tower.

4. FABRICATION CONSIDERATIONS

The performance feasibility for the proposed in-fiber structures is presented in Fig. 19 where one may see how a photonic crystal pre-form was filled with 7 randomly positioned golden wires and then drawn into a fiber using a drawing tower. The cross section presented in Fig. 19 is not the designed optimized structure that was discussed in this paper. Nevertheless it shows that existing fabrication capabilities may support the requirements for the realization of the proposed cable.

5. CONCLUSION

In this paper, we have presented a new type of cable design that can be fabricated using the technologies being developed for the realization of optical fibers. The central metallic core is shielded by 40 external wires. Silica is used as the isolation between the metallic wires. The silica region can also be used as the medium for the transmission of an optical carrier.

In this study, we saw that by properly designing a different electrical cable configuration, we are able to improve significantly the behavior of two of its principal drawbacks which are magnetic leakage and resistive heating. The proposed shield geometry is indeed more efficient concerning magnetic outflow which could be a source of disturbance for nearby systems. The material loss can be reduced as well using a single central wire. This outcome could have positive consequences on reducing the number of electronic amplifiers going along the proposed cable.

REFERENCES

1. Sali, S., "An improved model for the transfer impedance calculations of braided coaxial cables," *IEEE Transactions on Electromagnetic Compatibility*, Vol. 33, No. 2, May 1991.
2. Tiedemann, R., "Current flow in coaxial braided cable shields," *IEEE Transactions on Electromagnetic Compatibility*, Vol. 45, No. 3, Aug. 2003.
3. Knowles, E. D., "Cable shielding effectiveness testing," *IEEE Transactions on Electromagnetic Compatibility*, Vol. 16, No. 1, Feb. 1974.
4. Kley, T., "Optimized single-braided cable shields," *IEEE Transactions on Electromagnetic Compatibility*, Vol. 35, No. 1, Feb. 1993.
5. De Leo, R., G. Cerri, V. Mariani Primiani, and R. Botticelli, "A simple but effective way for cable shielding measurement," *IEEE Transactions on Electromagnetic Compatibility*, Vol. 41, No. 3, Aug. 1999.
6. Wheeler, H. A., "Formulas for the skin effect," *Proceedings of the I.R.E.*, Sep. 1942.
7. Wigington, R. L. and N. S. Nahman, "Transient analysis of coaxial cables considering skin effect," *Proceedings of the I.R.E.*, Feb. 1957.
8. Nahman, N. S., "A discussion on the transient analysis of coaxial cables considering high-frequency losses," *I.R.E. Transactions on Circuit Theory*, Jun. 1962.
9. Nahman, N. S. and D. R. Holt, "Transient analysis of coaxial cables using the skin effect approximation $A + B\sqrt{s}$," *IEEE Transactions on Circuit Theory*, Vol. 19, No. 5, Sep. 1972.
10. Calvez, L. C. and J. Le Bihan, "On numerical computation of functions related to transient response of capacitively loaded coaxial cables," *IEEE Transactions on Circuits and Systems*, Vol. 31, No. 9, Sep. 1984.
11. Le Bihan, J. and L. C. Calvez, "A new class of functions for transient analysis of coaxial cables terminated with parallel resistor and capacitor," *IEEE Transactions on Circuits and Systems*, Vol. 35, No. 5, May 1988.
12. Yen, C. S., Z. Fazarinc, and R. L. Wheeler, "Time-domain skin-effect model for transient analysis of lossy transmission lines," *Proceedings of the IEE*, Vol. 70, No. 7, Jul. 1982.
13. Colak, B., O. Cerezci, Z. Demir, M. Yazici, B. Turetken, and

I. Araz, "Calculation of leakage through apertures on coaxial cable braided screens," *IX-th International Conference on Mathematical Methods in Electromagnetic Theory, MMET'02*, 2002.

14. Benson, F. A., P. A. Cudd, and J. M. Tealby, "Leakage from coaxial cables," *IEEE Proceedings A*, Vol. 139, 1992.
15. Zalevsky, Z., A. K. George, F. Luan, G. Bouwmans, P. Dainese, C. Cordeiro, and N. July, "Photonic crystal in-fiber devices," *Opt. Eng.*, Vol. 44, 125003, 2005.
16. Williamson, R. C. and R. D. Esman, "RF Photonics," *J. Lightwave Technol.*, Vol. 26, 1145–1153, 2008.
17. Lin, C. T., J. Chen, P. C. Peng, C. F. Peng, W. R. Peng, B. S. Chiou, and S. Chi, "Hybrid optical access network integrating fiber-to-the-home and radio-over-fiber systems," *IEEE Photonics Technology Letters*, Vol. 19, No. 8, 610–612, Apr. 2007.
18. Yashchyshyn, Y., S. Malyshev, A. Chizh, P. Bajurko, and J. Modelski, "Study of active integrated photonic antenna," *Proc. EuCAP'09*, 3507–3510, Mar. 2009.
19. Chang, C. H., W. C. Liu, P. C. Peng, H. H. Lu, P. Y. Wu, and J. B. Wang, "Hybrid cable television and orthogonal-frequency-division-multiplexing transport system basing on single wavelength polarization and amplitude remodulation schemes," *Opt. Lett.*, Vol. 36, 1716–1718, 2011.
20. O'brien, D. G., "Hybrid fiber optic/electrical cable and connector," US Patent 4,896,939, 1987.